

Multipartite entanglement of three trapped ions in a cavity and W- State generation

S. Shelly Sharma* and Eduardo de Almeida

Depto. de Física, Universidade Estadual de Londrina, Londrina 86051-990, PR Brazil

Naresh K. Sharma

Depto. de Matematica, Universidade Estadual de Londrina, Londrina 86051-990, PR Brazil

A scheme to generate three qubit maximally entangled W-states, using three trapped ions interacting with red sideband tuned single mode field of a high finesse cavity, is proposed. For the cavity field initially prepared in a number state, the probability of generating three ion W-state is calculated. By using the ion-cavity coupling strengths achieved in experimental realizations, the interaction time needed for W-state generation is found to be of the order of 10μ sec. It is found that for a fixed number of photons in the cavity the nature of entanglement of ionic internal states can be manipulated by appropriate choice of initial state phonon number.

The ionic qubits in W-like state are found to be entangled to cavity photons. Analytical expressions for global negativity and partial K -way negativities ($K = 2$ to 4) are obtained to study the evolution of entanglement distribution as a function of interaction parameter. Reversible entanglement exchange between different entanglement modes is observed. For specific values of interaction parameter, the three ions and photon-phonon system are found to have four partite entanglement, generated by 2-way and 3-way correlations.

I. INTRODUCTION

Interest in manipulation of multipartite quantum states is motivated by the possible use in quantum communication [1], quantum dense coding [2] and quantum teleportation [3]. Advances in experimental techniques of trapping, cooling, and manipulation of internal states of ions through interaction with external lasers [4, 5, 6] have made the generation of maximally entangled states [7] a reality. While single atoms and ions, with long-lived internal states, are suitable for storing quantum information, the photonic qubits serve as fast and reliable carriers to transport quantum information over long distances. Cirac et al. [8] considered the possibility of using photonic channels to interconnect high finesse cavities with single trapped ions inside. It was shown in ref. [9], that the composite quantum system with a single trapped two-level ion interacting with a quantized light field in single-mode cavity evolves into maximally entangled three-particle Greenberger-Horne-Zeilinger state. A different scheme to generate three qubit maximally entangled GHZ state, using a trapped ion interacting with a resonant external laser and sideband tuned single mode of a cavity field has been proposed in ref. [10] and the decoherence process of this three qubit system examined [11]. Experimentally successful efforts in this direction [12, 13, 14], have demonstrated coherent coupling of electronic and motional states of a single trapped Ca^+ ion to single field mode of a high finesse cavity. In the experiment of ref. [12], a Ca^+ ion in a RF-Paul trap was placed with high precision at an arbitrary position in the standing wave field of a near-confocal resonator for several hours of interaction time. Since the size of the cavity is large compared to the wavelength of standing wave, a large number of nodes and antinodes of the standing wave are formed inside the cavity. The electromagnetically induced transparency (EIT) method used in the work of Morigi et. al. [15] and Roos et al. [16], could make possible the initialization of motional states of ion strings in a cavity. These experiments open the possibility that more than one trapped ions may be cooled down to their lowest vibrational states and interact with the quantized cavity field. A string of ions in the same trap with the center of mass in a definite motional mode may, likewise, be prepared inside a cavity. In this article, we propose a scheme in which three two-level trapped ions are cooled inside a high finesse cavity to generate multipartite entangled states through coherent coupling of their electronic and vibrational states to the standing wave cavity field. For the cavity field initially prepared in a number state, we obtain conditions on the interaction parameters to generate states in which three ions in W like state are entangled to cavity photons. Tessier et al. [17] have investigated the multipartite entanglement of two two-level atoms, generated by resonant coupling to a single mode of the electromagnetic field. The resulting physical system corresponds to the two-atom Tavis-Cummings model [18]. Our system is similar to that of ref. [17] in that the

*Electronic address: shelly@uel.br

entanglement between the ions arises not through direct interaction between the ions, but through their coupling to the phonon-photon system. We have not considered the effects of spontaneous decay, decoherence of motional states and cavity losses in this article. The object of studying a closed system, without decoherence effects, is to have a clear picture of dynamics of quantum correlations. The entanglement of mixed multipartite states resulting due to decoherence is not so well understood. The memory qubits (ionic internal states) are known to have a coherence time of the order of seconds and even minutes (magnetically insensitive transitions). The success of experiments with a single ion indicates, that the motional decoherence caused by trap fluctuations or environment noise is negligible on the time-scale of state generation and photon qubit coherence of the order of miliseconds. The decoherence caused by the implementation of the scheme itself needs to be studied theoretically for the three ion case though such studies for single ion case have been done in refs. [11, 19].

Multipartite entanglement is a useful resource for implementation of quantum information processing protocols [20]. To retrieve information about the entanglement of a group of K ($2 \leq K \leq 4$) subsystems of the composite system, we use the global negativity and the partial K -way negativities. For analyzing the entanglement dynamics, we have considered the vibrational phonons and cavity photons to constitute a single quantum system. Negativity [21, 22, 23], based on Peres Horodecki [24, 25] criterion, has been shown to be an entanglement monotone [26]. The K -way negativity refers to the negativity of a partial transpose constructed by imposing specific constraints during transposition. The coherences of a multipartite composite system having N subsystems can be quantified by K -way negativities [27] ($2 \leq K \leq N$). Partial K -way negativity is the contribution of a specific K -way partial transpose to global negativity. For canonical states, the partial K -way negativities measure the genuine K -partite entanglement of the system [28, 29]. Genuine K -partite entanglement refers to K -partite entanglement due to correlations similar to those present in a GHZ-like state of K subsystems. Loss of a single subsystem destroys this type of entanglement completely, leaving no residual entanglement. We have obtained analytical expressions for partial K -way negativities with respect to photon-phonon state and internal states of ions. The advantage of using partial K -way negativities lies in the fact that the entanglement between parts of a composite system is obtained from the full state operator, without state reduction. With the cavity prepared initially in a Fock state, the entanglement of ionic internal states depends strongly on the choice of phonon number at $t = 0$. Extra control on qubit state manipulation, gained by coupling the vibrational modes to the cavity field [13, 14], is an advantage for successful implementation of quantum gates.

The vector space and system Hamiltonian are discussed in section II. Analytical expressions for the state of the system at current time, with the three ions prepared in their respective (i) ground states, and (ii) excited states, are presented in section III. The role of initial state center of mass quanta in state manipulation and the time evolution of W-state generation probabilities is also discussed in section III. In section IV, the entanglement dynamics of ions, phonons and photons is investigated. The Global and partial K -way negativities, used to study the entanglement distribution in the composite system, are defined and calculated analytically as well as numerically for special initial state preparations of the system. We discuss, briefly, the information gained from the dynamics of global and partial K -way negativities in section V, followed by the conclusions in section VI.

II. THE MODEL

Consider three two level trapped cold ions vibrating with trap frequency ν inside a high finesse cavity. The frequency of standing wave cavity field is ω_c and ions are well separated from each other so that no dipole interaction takes place between the ions. The free Hamiltonian of the system composed of internal states of ions, the vibrational state of center of mass and the state of standing wave cavity field is given by

$$\hat{H}_0 = \hbar\nu \left(\hat{a}^\dagger \hat{a} + \frac{1}{2} \right) + \hbar\omega_c \hat{b}^\dagger \hat{b} + \frac{\hbar\omega_0}{2} \sum_{j=1}^3 \hat{\sigma}_z^{(j)}, \quad (1)$$

where $\hat{a}^\dagger(\hat{a})$ and $\hat{b}^\dagger(\hat{b})$ are the creation(annihilation) operators for vibrational phonons and cavity field photons, respectively. Eigen states of Pauli operator $\hat{\sigma}_z^{(j)}$ model the internal states of the j^{th} two-level ion ($j = 1, 2, 3$) with energy splitting $\hbar\omega_0$. We define the total spin operators as $\hat{\sigma}_k = \sum_{j=1}^3 \hat{\sigma}_k^{(j)}$, where $k = (z, +, -)$ and use the eigenvectors of $\hat{\sigma}^2$ and $\hat{\sigma}_z$ to represent the three ion internal states. The ionic internal states in product basis are labelled as $|\sigma_z^{(1)} \sigma_z^{(2)} \sigma_z^{(3)}\rangle$ ($\sigma_z^{(j)} = -1$ or $+1$). The coupled basis vectors are $|\sigma, \sigma_z\rangle$, where the label $\sigma (= 2s)$ refers to the eigenvalue of σ^2 given by $\sigma(\sigma + 2)$. The computational basis states, on the other hand, read as $|i_1, i_2, i_3\rangle$, where $i_j = 0$ for atom in ground state and $i_j = 1$ for atom in the excited state.

The interaction of cold ions, located at the node of the standing wave, with the quantized cavity field is given by

$$\hat{H}_I = \hbar g(\hat{\sigma}_+ + \hat{\sigma}_-)(\hat{b}^\dagger + \hat{b}) \sin[\eta(\hat{a}^\dagger + \hat{a})], \quad (2)$$

g being the ion-cavity coupling constant and η the Lamb-Dicke parameter. The interaction picture Hamiltonian obtained by applying the unitary transformation $\hat{U}_I = \exp(-i\hat{H}_0 t/\hbar)$ is a complex looking operator [30]. However, with the cavity coupled to red sideband of ionic vibrational motion ($\omega_0 - \omega_c = \nu$), the relevant part of \hat{H}_I in the rotating-wave approximation and Lamb-Dicke limit ($\eta \ll 1$) reduces to

$$\hat{H}_{II} = \hbar g \eta [\hat{\sigma}_+ \hat{b} \hat{a} + \hat{\sigma}_- \hat{b}^\dagger \hat{a}^\dagger]. \quad (3)$$

The possible values of σ for three ions are 3, 1, 1, there being two distinct internal configurations that allow $\sigma = 1$. The matrix T that transforms from the computational basis to the coupled basis is given by

$$T = \begin{pmatrix} 1 & 0 & 0 & 0 & 0 & 0 & 0 & 0 \\ 0 & \frac{1}{\sqrt{3}} & \frac{1}{\sqrt{3}} & 0 & \frac{1}{\sqrt{3}} & 0 & 0 & 0 \\ 0 & 0 & 0 & \frac{1}{\sqrt{3}} & 0 & \frac{1}{\sqrt{3}} & \frac{1}{\sqrt{3}} & 0 \\ 0 & 0 & 0 & 0 & 0 & 0 & 0 & 1 \\ 0 & \frac{1}{\sqrt{6}} & \frac{1}{\sqrt{6}} & 0 & -\sqrt{\frac{2}{3}} & 0 & 0 & 0 \\ 0 & 0 & 0 & \sqrt{\frac{2}{3}} & 0 & \frac{-1}{\sqrt{6}} & \frac{-1}{\sqrt{6}} & 0 \\ 0 & \frac{1}{\sqrt{2}} & \frac{-1}{\sqrt{2}} & 0 & 0 & 0 & 0 & 0 \\ 0 & 0 & 0 & 0 & 0 & \frac{1}{\sqrt{2}} & \frac{-1}{\sqrt{2}} & 0 \end{pmatrix}. \quad (4)$$

The computational basis vectors are taken in the order $|000\rangle, |100\rangle, |010\rangle, |110\rangle, |001\rangle, |101\rangle, |011\rangle$, and $|111\rangle$, while the ordering of coupled basis vectors is $|3, -3\rangle, |3, -1\rangle, |3, 1\rangle, |3, 3\rangle, |1, -1\rangle_1, |1, 1\rangle_1, |1, -1\rangle_2, |1, 1\rangle_2$. The subscript in $|1, \pm 1\rangle_{1,2}$ distinguishes the states with same value of σ but different internal configurations.

The product state of the composite system looks like $|\sigma, \sigma_z\rangle \otimes |m, n\rangle$, where m is the number of center of mass vibrational quanta and n is the number of cavity field photons. The advantage of working in a coupled basis stems from the fact that the Hamiltonian of Eq. (3) does not connect states with different values of σ . If the initial state is an eigenstate of $\hat{\sigma}^2$ with eigenvalue $\sigma_I(\sigma_I + 2)$, the system evolves into a linear combination of states of the type $|\sigma_I, \sigma_z, m, n\rangle$ with $-\sigma_I \leq \sigma_z \leq \sigma_I$.

For $\sigma_I = 3$ the Hamiltonian (Eq. (3)) in the basis $|3, 3\rangle \otimes |m-2, n-2\rangle, |3, 1\rangle \otimes |m-1, n-1\rangle, |3, -1\rangle \otimes |m, n\rangle$, and $|3, -3\rangle \otimes |m+1, n+1\rangle$ is written as

$$H_{II}(\sigma = 3) = \begin{pmatrix} 0 & \sqrt{2}A_{mn} & 0 & 0 \\ \sqrt{2}A_{mn} & 0 & \sqrt{2}B_{mn} & 0 \\ 0 & \sqrt{2}B_{mn} & 0 & \sqrt{2}C_{mn} \\ 0 & 0 & \sqrt{2}C_{mn} & 0 \end{pmatrix}, \quad (5)$$

where

$$A_{mn} = \hbar g \eta \sqrt{\frac{3}{2}(m-1)(n-1)}, B_{mn} = \hbar g \eta \sqrt{2mn}, \quad (6)$$

and

$$C_{mn} = \hbar g \eta \sqrt{\frac{3}{2}(m+1)(n+1)}. \quad (7)$$

Defining

$$\mu = (A_{mn}^2 + B_{mn}^2 + C_{mn}^2), \text{ and } \beta = \sqrt{\mu^2 - 4A_{mn}^2 C_{mn}^2},$$

the eigenvalues of H , in units of $\hbar g \eta$, are

$$\begin{aligned} E_1 &= -\sqrt{\mu - \beta}, & E_2 &= \sqrt{\mu - \beta}, \\ E_3 &= -\sqrt{\mu + \beta}, & E_4 &= \sqrt{\mu + \beta}. \end{aligned} \quad (8)$$

The unitary matrix \hat{U} that diagonalizes $H_{II}(\sigma = 3)$, $(H_{II}(\sigma = 3)|\phi_i\rangle = E_i|\phi_i\rangle, (i = 1, 4))$ is given by

$$\hat{U}(\sigma = 3) = \begin{pmatrix} \sqrt{\frac{\beta+\mu_2}{4\beta}} & -\sqrt{\frac{\beta-\mu_1}{4\beta}} & -\sqrt{\frac{\beta-\mu_2}{4\beta}} & \sqrt{\frac{\beta+\mu_1}{4\beta}} \\ -\sqrt{\frac{\beta+\mu_2}{4\beta}} & -\sqrt{\frac{\beta-\mu_1}{4\beta}} & \sqrt{\frac{\beta-\mu_2}{4\beta}} & \sqrt{\frac{\beta+\mu_1}{4\beta}} \\ -\sqrt{\frac{\beta-\mu_2}{4\beta}} & \sqrt{\frac{\beta+\mu_1}{4\beta}} & -\sqrt{\frac{\beta+\mu_2}{4\beta}} & \sqrt{\frac{\beta-\mu_1}{4\beta}} \\ \sqrt{\frac{\beta-\mu_2}{4\beta}} & \sqrt{\frac{\beta+\mu_1}{4\beta}} & \sqrt{\frac{\beta+\mu_2}{4\beta}} & \sqrt{\frac{\beta-\mu_1}{4\beta}} \end{pmatrix}, \quad (9)$$

where $\mu_1 = \mu - 2A_{mn}^2$ and $\mu_2 = \mu - 2C_{mn}^2$.

Starting from a given initial state, $|\sigma_z^{(1)}\sigma_z^{(2)}\sigma_z^{(3)}\rangle \otimes |m, n\rangle$, of the system, the time evolution in interaction picture is obtained by applying the transformation $\exp(-i\hat{H}_{II}t/\hbar)$. An internal state of ions may be rewritten in terms of the coupled basis states as

$$|\sigma_z^{(1)}, \sigma_z^{(2)}, \sigma_z^{(3)}\rangle_j = \sum_i T_{ji}^\dagger |\sigma, \sigma_z\rangle_i. \quad (10)$$

The state $|\sigma, \sigma_z\rangle \otimes |m, n\rangle_i$ of the composite system with m vibrational quanta and n photons may, in turn, be expanded in terms of eigen states of $H_{II}(\sigma)$ as

$$|\sigma, \sigma_z\rangle \otimes |m, n\rangle_i = \sum_k U_{ik}^\dagger(\sigma) |\phi_k\rangle. \quad (11)$$

We recall that the matrix T operates on the internal states of the two-level atom, while \hat{U} operates in the composite Hilbert space formed by internal states, cavity field states and the state of vibrational motion. The state of the system at instant t is given by

$$\Psi(t) = \sum_i \sum_k T_{ji}^\dagger U_{ik}^\dagger(\sigma) \exp(-i\lambda_k g \eta t) |\phi_k\rangle. \quad (12)$$

To go back to the computational basis we use the inverse transformation. The state obtained is in the interaction picture and we go to Schrödinger picture by the transformation $\Psi_S(t) = e^{-\frac{iH_0 t}{\hbar}} \Psi(t)$. As the state of the composite system evolves, the internal states of ions, the cavity field state and the state of vibrational motion become entangled.

III. THE COMPOSITE SYSTEM STATE

A. Initial state, $\Psi_{m+1, n+1}(0) = |000\rangle \otimes |m+1, n+1\rangle$

Consider the three ions in their ground states with the center of mass motion cooled down to a state with $m+1$ vibrational quanta. Photon field set to a fixed detuning is injected in to the cavity such that the cavity state is an $n+1$ photon Fock state at $t=0$. The analytical expression for the state of the system at current time t is found to be

$$\begin{aligned} \Psi_{m+1, n+1}(t) = & a_0(t)|000\rangle \otimes |m+1, n+1\rangle + a_1(t)|W_1\rangle \otimes |m, n\rangle \\ & + a_2(t)|W_2\rangle \otimes |m-1, n-1\rangle + a_3(t)|111\rangle \otimes |m-2, n-2\rangle \end{aligned} \quad (13)$$

where $|W_1\rangle = \frac{|100\rangle + |001\rangle + |010\rangle}{\sqrt{3}}$ and $|W_2\rangle = \frac{|110\rangle + |101\rangle + |011\rangle}{\sqrt{3}}$ are W states with one and two excited ions, respectively. The coefficients $a_i(t)$, $i = 0$ to 3 ,

$$a_0(t) = \frac{e^{-i\omega_1 t}}{2\beta} \left((\beta - \mu_2) \cos(\sqrt{(\mu + \beta)g\eta t}) + (\beta + \mu_2) \cos(\sqrt{(\mu - \beta)g\eta t}) \right), \quad (14)$$

$$\begin{aligned} a_1(t) = & -\frac{ie^{-i\omega_1 t}}{2\beta} \left(\sqrt{(\beta - \mu_2)(\beta + \mu_1)} \sin(\sqrt{(\mu + \beta)g\eta t}) \right. \\ & \left. + \sqrt{(\beta + \mu_2)(\beta - \mu_1)} \sin(\sqrt{(\mu - \beta)g\eta t}) \right), \end{aligned} \quad (15)$$

$$a_2(t) = \frac{e^{-i\omega_1 t} \sqrt{\beta^2 - \mu_2^2}}{2\beta} \left(\cos(\sqrt{(\mu + \beta)g\eta t}) - \cos(\sqrt{(\mu - \beta)g\eta t}) \right), \quad (16)$$

and

$$a_3(t) = -\frac{ie^{-i\omega_1 t}}{2\beta} \left(\sqrt{(\beta - \mu_2)(\beta - \mu_1)} \sin(\sqrt{(\mu + \beta)g\eta t}) - \sqrt{(\beta + \mu_2)(\beta + \mu_1)} \sin(\sqrt{(\mu - \beta)g\eta t}) \right), \quad (17)$$

satisfy the normalization condition $\sum_{i=0}^3 |a_i(t)|^2 = 1$. The frequency $\omega_1 = \nu(m + \frac{3}{2}) + \omega_c(n + 1) - \frac{3\omega_0}{2}$, refers to zero point energy of the initial state. The probability amplitude $a_2(t)$ is zero whenever $\cos(\sqrt{(\mu + \beta)g\eta t}) = \cos(\sqrt{(\mu - \beta)g\eta t})$. For values of t such that $\cos(\sqrt{(\mu + \beta)g\eta t}) = \cos(\sqrt{(\mu - \beta)g\eta t}) = \pm 1$, the composite system state is a separable state. When the condition $\sin(\sqrt{(\mu + \beta)g\eta t}) = \sin(\sqrt{(\mu - \beta)g\eta t}) = \pm 1$ is satisfied, the composite system is found to be in the state

$$\Psi_{m+1,n+1}^{W_1}(t) = a_1(t)|W_1\rangle \otimes |m, n\rangle + a_3(t)|111\rangle \otimes |m - 2, n - 2\rangle, \quad (18)$$

where the probability amplitudes

$$a_1(t) = -\frac{ie^{-i\omega_1 t}}{2\beta} \left(\sqrt{(\beta - \mu_2)(\beta + \mu_1)} + \sqrt{(\beta + \mu_2)(\beta - \mu_1)} \right), \quad (19)$$

$$a_3(t) = -\frac{ie^{-i\omega_1 t}}{2\beta} \left(\sqrt{(\beta - \mu_2)(\beta - \mu_1)} - \sqrt{(\beta + \mu_2)(\beta + \mu_1)} \right), \quad (20)$$

depend strongly on the initial state photon and phonon number. The three ions in W_1 -like state are found to be entangled to photon-phonon state, constituting a state having four-partite entanglement.

The probabilities $P_i(\tau)$ of finding i number of ions ($i = 0$ to 3) in excited state are plotted as a function of variable τ in figure (1), for the choice $m = n = 2$. The value of parameter $\tau = g\eta t$ is determined by the cavity ion coupling strength, Lamb Dicke parameter and the interaction time. We notice that for $\tau \approx 3\pi/4$ the system is found to be in a separable state and for $\tau \approx 3\pi/8$ in state $\Psi_{3,3}^{W_1}$, with $P_1(\tau) \approx 0.75$, and $P_3(\tau) \approx 0.25$.

B. Initial state, $\Phi_{m-2,n-2}(0) = |111\rangle \otimes |m - 2, n - 2\rangle$

When all three ions are in their excited states at $t = 0$, the center of mass prepared in a state with $m - 2$ vibrational quanta, and the cavity in $n - 2$ photon Fock state, the state of the composite quantum system at current time is found to be

$$\begin{aligned} \Phi_{m-2,n-2}(t) = & a_3(t)|000\rangle \otimes |m + 1, n + 1\rangle + a_2(t)|W_1\rangle \otimes |m, n\rangle \\ & + a_1(t)|W_2\rangle \otimes |m - 1, n - 1\rangle + a_0(t)|111\rangle \otimes |m - 2, n - 2\rangle. \end{aligned} \quad (21)$$

The maximum number of coupled basis states populated by the ions as the interaction time increases is four, independent of the initial state photon or phonon number. Recalling that for interaction time such that $\sin(\sqrt{(\mu + \beta)g\eta t}) = \sin(\sqrt{(\mu - \beta)g\eta t}) = \pm 1$, the probability amplitude $a_0(t) = a_2(t) = 0$, we find the three ions in W_2 -like state entangled to photon-phonon state such that

$$\Phi_{m-2,n-2}^{W_2}(t) = a_3(t)|000\rangle \otimes |m + 1, n + 1\rangle + a_1(t)|W_2\rangle \otimes |m - 1, n - 1\rangle, \quad (22)$$

with probability amplitudes $a_1(t)$ and $a_3(t)$ given by Eqs(19) and (20) respectively. Figure (2) displays the probabilities $P_i(\tau)$ ($i = 0$ to 3) as a function of variable τ for the choice $m = 2, n = 2$ at $t = 0$. The initial state preparation in this case involves cooling the center of mass motion to zero phonon mode with ions in ground state and the cavity in vacuum state. The internal states of three ions can now be prepared in the excited state through controlled resonant interaction with external lasers. The ion's state is well preserved due to the long lifetime (~ 1 s). We observe that the composite system periodically returns to initial separable state with a period of $t \approx \frac{3\pi}{4g\eta}$. The black arrows point out the $P_2(\tau)$ corresponding to state $\Phi_{00}^{W_2}(t)$.

C. Quantum state control and the number of vibrational quanta

The maximum number of coupled basis states populated by the ions can be controlled by the number of initial state photon and phonon number. With the center of mass prepared initially in one phonon mode ($m + 1 = 1$), and the cavity having one or more photons ($n + 1 \geq 1$), the composite system is found to be in the state

$$\begin{aligned} \Psi_{1,n+1}(t) = & \cos\left(\sqrt{3(n+1)}g\eta t\right)e^{-i\omega_1 t}|000\rangle \otimes |1, n+1\rangle \\ & - i \sin\left(\sqrt{3(n+1)}g\eta t\right)e^{-i\omega_1 t}|W_1\rangle \otimes |0, n\rangle, \end{aligned} \quad (23)$$

whereas for ionic center of mass in zero phonon mode, the state of the system remains unchanged. The minimum interaction time needed to get the three ion W_1 state generation probability peak is $t_{\min} = \frac{\pi}{2g\eta\sqrt{3(n+1)}}$. Deterministic coupling of ion's quantized vibration in the trap to the cavity mode, has been demonstrated by Mundt et al. [13]. For cavity ion coupling strength $g = 8.95$ MHz, Lamb Dicke parameter value $\eta = 0.01$ and cavity prepared in single photon state at $t = 0$, we obtain $t_{\min} = \frac{\pi}{2g\eta\sqrt{3}} = 10.133\mu$ sec. This is the simplest setting for generating three ion W state with a single ion in excited state. The three ion $|W_1\rangle$ state generation time can be decreased by increasing the number of initial state photons in the cavity. The increase in cavity decay probability with increase in photon number is likely to reduce the $|W_1\rangle$ state generation probability and must be carefully accounted for.

For the initial state preparation with $m + 1 = 2$ and $n + 1 \geq 2$ the state of the system at current time is

$$\begin{aligned} \Psi_{2,n+1}(t) = & \frac{e^{-i\omega_1 t}}{(5n+3)} \left((3n+3) \cos\left(\sqrt{2(5n+3)}g\eta t\right) + 2n \right) |000\rangle \otimes |2, n+1\rangle \\ & - ie^{-i\omega_1 t} \sqrt{\frac{(3n+3)}{(5n+3)}} \sin\left(\sqrt{2(5n+3)}g\eta t\right) |W_1\rangle \otimes |1, n\rangle \\ & + \frac{e^{-i\omega_1 t} \sqrt{6n(n+1)}}{(5n+3)} \left(\cos\left(\sqrt{2(5n+3)}g\eta t\right) - 1 \right) |W_2\rangle \otimes |0, n-1\rangle. \end{aligned} \quad (24)$$

The period for the system to return to initial separable state is $t_p = \frac{2\pi}{g\eta\sqrt{2(5n+3)}}$. At $t_w = \frac{\pi}{g\eta\sqrt{2(5n+3)}}$, we have ions in W_2 -like state coupled to photon-phonon system in state

$$\Psi_{2,n+1}(t) = \frac{e^{-i\omega_1 t}(n+3)}{(5n+3)} |000\rangle \otimes |2, n+1\rangle + \frac{e^{-i\omega_1 t} 2\sqrt{6n(n+1)}}{(5n+3)} |W_2\rangle \otimes |0, n-1\rangle. \quad (25)$$

We notice that the maximum probability of finding the state $|W_2\rangle$ increases with n , approaching $\cong \frac{24}{25}$ in the large n limit. When initial state phonon and photon number is greater or equal to three, all the four coupled basis vector states seen in eq. (13) can be reached.

D. W- state Generation probabilities

Three qubit W-states are extremely useful for implementing various communication protocols, quantum state transport and quantum gates. These states do not have genuine tripartite entanglement, but maximal pairwise entanglement. For these states, global negativity and partial two way negativity is non zero, while the partial three way negativity is zero [31], which is equivalent to the three tangle [32] being zero. The tripartite entanglement of the state is due bipartite correlations. We label the three ions as subsystems A , B , C , and consider the phonons and photons to constitute a single quantum system D . The reduced state operator for the ions

$$\rho_{m+1n+1}^{ABC}(t) = \text{tr}_D(|\Psi_{m+1,n+1}(t)\rangle \langle \Psi_{m+1,n+1}(t)|)$$

obtained by tracing over the vibrational and cavity state degrees of freedom is a mixed state given by

$$\rho_{m+1n+1}^{ABC}(t) = |a_0(t)|^2 |000\rangle \langle 000| + |a_1(t)|^2 |W_1\rangle \langle W_1| + |a_2(t)|^2 |W_2\rangle \langle W_2| + |a_3(t)|^2 |111\rangle \langle 111|. \quad (26)$$

The probability $P_1(\tau)$ and $P_2(\tau)$ in figure (1), are the probabilities of finding the three ions in the state $|W_1\rangle$ and $|W_2\rangle$ for the choice $m + 1 = n + 1 = 3$. We notice that for $t = \frac{3\pi}{8g\eta}$, $P_0(\tau) = P_2(\tau) = 0$, $P_1(\tau)$ shows a peak and $P_3(\tau)$ is finite.

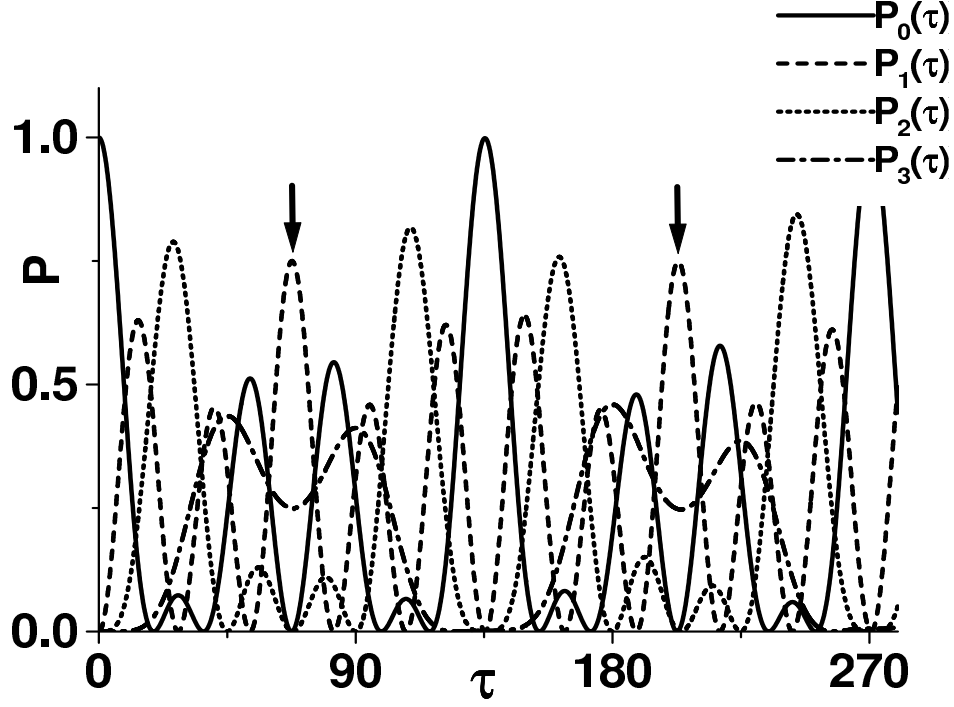


FIG. 1: The probabilities P_i , $i = 0$ to 3 versus $\tau (= g\eta t)$ for the initial state $|000, 3, 3\rangle$.

The choice $m = n = 0$, in Eq. (13) yields

$$\rho_{11}^{ABC}(t) = \cos^2(\sqrt{3}g\eta t) |000\rangle\langle 000| + \sin^2(\sqrt{3}g\eta t) |W_1\rangle\langle W_1|,$$

with deterministic $|W_1\rangle$ state generation at $t = \frac{k\pi}{2g\eta\sqrt{3}}$, where k is an odd integer.

For the choice $m = n = 1$, in Eq. (13) we get

$$\begin{aligned} \rho_{22}^{ABC}(t) = & \left(\frac{3}{4} \cos(4g\eta t) + \frac{1}{4} \right)^2 |000\rangle\langle 000| + \frac{3}{4} \sin^2(4g\eta t) |W_1\rangle\langle W_1| \\ & + \frac{3}{16} (\cos(4g\eta t) - 1)^2 |W_2\rangle\langle W_2|. \end{aligned} \quad (27)$$

For an interaction time of $t = \frac{k\pi}{8g\eta}$, $k = 1, 3, 5, \dots$, the ionic state $|W_1\rangle$ is found with a probability of 75% in the state

$$\rho_{22}^{ABC} \left(\frac{k\pi}{8g\eta} \right) = \frac{1}{16} |000\rangle\langle 000| + \frac{3}{4} |W_1\rangle\langle W_1| + \frac{3}{16} |W_2\rangle\langle W_2|, \quad (28)$$

whereas the probability of finding the three ions in state $|W_2\rangle$ is maximized for $t = \frac{k\pi}{4g\eta}$, with the reduced state operator reading as

$$\rho_{22}^{ABC} \left(\frac{k\pi}{4g\eta} \right) = \frac{1}{4} |000\rangle\langle 000| + \frac{3}{4} |W_2\rangle\langle W_2|. \quad (29)$$

For $t = \frac{k\pi}{4g\eta}$ with $k = 0, 2, 4, \dots$ the three ions are found in their ground states. The three ion state is a mixed state, $\frac{1}{3} |W_1\rangle\langle W_1| + \frac{2}{3} |W_2\rangle\langle W_2|$, for $g\eta t$ values such that $\cos(4g\eta t) = -\frac{1}{3}$.

The three ion state operator ($\rho_{m-2,n-2}^{ABC}(t) = \text{tr}_D(|\Phi_{m-2,n-2}(t)\rangle\langle\Phi_{m-2,n-2}(t)|)$), reads as

$$\rho_{m-2,n-2}^{ABC}(t) = |a_3(t)|^2 |000\rangle\langle 000| + |a_2(t)|^2 |W_1\rangle\langle W_1| + |a_1(t)|^2 |W_2\rangle\langle W_2| + |a_0(t)|^2 |111\rangle\langle 111|. \quad (30)$$

For $m = n = 2$, the W_2 state population probability at peak value is found to be 75% as seen in figure (2). The probability of populating W_1 state is, relatively, small.

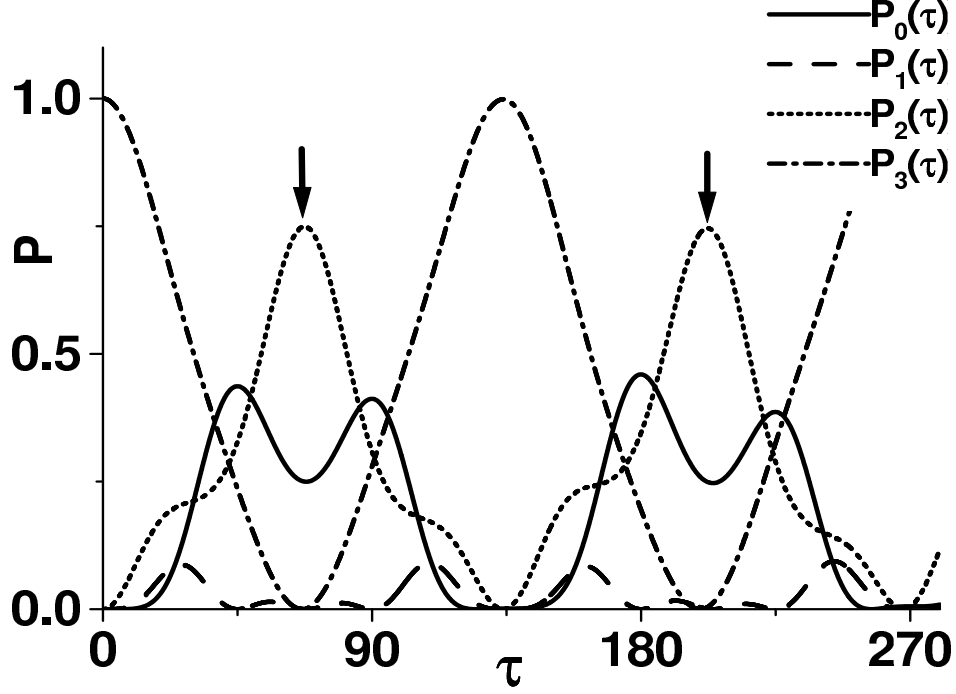


FIG. 2: The probabilities P_i , $i = 0$ to 3 versus $\tau (= g\eta t)$ for the initial state: $|111, 0, 0\rangle$.

IV. ENTANGLEMENT OF IONIC QUBITS AND PHOTONS

The entanglement of ionic memory qubits in W-like state to cavity photons is an extremely interesting and useful aspect of the proposed scheme. Entangled cavity photons can transport information to a remote cavity in a fast and reliable way. For analyzing the entanglement dynamics, we consider the $(m + 1 - i)$ phonons and $(n + 1 - i)$ photons to constitute a single quantum system in the space spanned by vectors $|i\rangle$ ($i = 0$ to 3), where $|i\rangle$ represents the state $|m + 1 - i, n + 1 - i\rangle$. Furthermore, the ground and excited state of an ion represent logical bits $|0\rangle$ and $|1\rangle$, respectively. The composite state of Eq. (13), in logical basis, reads as

$$\begin{aligned} \Psi_{m+1,n+1}(t) = & a_0(t)|0000\rangle + a_1(t) \left(\frac{|1001\rangle + |0101\rangle + |0011\rangle}{\sqrt{3}} \right) \\ & + a_2(t) \left(\frac{|1102\rangle + |1012\rangle + |0112\rangle}{\sqrt{3}} \right) + a_3(t)|1113\rangle. \end{aligned} \quad (31)$$

Labelling the three ions as A, B, C and cavity field plus phonon state as subsystem D , the possible bipartite partitions of the system are $A - BCD$, $B - ACD$, $C - ABD$, $D - ABC$, $AB - CD$, $AC - BD$, and $AD - BC$. We notice that the ionic state is symmetrical with respect to interchange of a pair of qubits. As such distinct partitions are reduced to $A - BCD$, $D - ABC$, and $AB - CD$. The state is in bi-orthogonal Schmidt form for qubits A, B, C and subsystem D . Quantifying or even detecting the entanglement of the composite system with four subsystems is a fairly complex task. The four subsystems may have four-partite GHZ state like correlations, or 4-partite entanglement resulting from bipartite entanglement between the subsystems. On tracing over anyone of the subsystems, 4-party GHZ like entanglement is destroyed, but the three remaining subsystems may have tripartite GHZ like entanglement or W-like entanglement. While the GHZ-like tripartite entanglement is completely destroyed on tracing over one subsystem out of the three, the reduced bipartite mixed state may still have bipartite entanglement (provided that the tripartite system had W-like entanglement). The entanglement distribution in the pure state of the composite system determines the entanglement available simultaneously to all the four parties, three selected parties or a pair of subsystems. In particular, the nature, distribution and dynamics of entanglement involving the memory qubits (trapped ions ABC) and photons is of special interest if the system is part of a quantum network.

A. Peres [24] was the first to observe that a partial transpose of density matrix associated with a separable state of a bipartite system is still a valid density matrix and thus positive (semi) definite. Horodecki et al. [25] proved that a

positive partial transpose (PPT) was a necessary and sufficient condition for separability of a state if the dimension of the Hilbert space does not exceed six. A negative partial transpose is a clear signature of entanglement. Negativity [21, 22, 23] based on Peres Horodecki PPT criterion has been shown to be an entanglement monotone [26]. In a recent article [28], we introduced 2-way and 3-way negativities to discuss the entanglement of three qubit states. In refs. [27, 29], a characterization of multipartite quantum states having N subsystems, based on partial K -way negativities has been proposed. The K -way partial transpose with respect to a subsystem is constructed from the state operator by imposing specific constraints on the matrix elements involving the states of K subsystems of multipartite composite system. It has been shown that the partial transpose of density matrix of an N -partite system, with respect to a given subsystem, can be written as a sum of K -way partial transposes where $2 \leq K \leq N$. Contribution to negativity due to a K -way partial transpose is easily calculated. The K -way negativity ($2 \leq K \leq N$), defined as the negativity of K -way partial transpose, quantifies the K -way coherences of the composite system. In contrast with the entropic measures of entanglement, where a reduced state operator is used to obtain information about the correlations between parts of a composite system, the partial K -way negativities are calculated from the state operator of the composite system itself. The negativity of global partial transpose remains invariant under local operations and classical communication (LOCC), however, the partial K -way negativities may increase or decrease under LOCC at the cost of each other. The partial K -way negativities show the entanglement distribution in different parts of the system in a given state. While the total entanglement in a composite system can not be increased by local operations, the entanglement distribution can be changed by local operations. In this section we investigate the entanglement dynamics of the composite system state by using the global negativity to detect the entanglement, and partial K -way negativities to determine the entanglement distribution amongst different subsystems.

A. Definition of Global and K -way negativities

The global partial transpose $\hat{\rho}_G^{TA}$ of four-party state operator $\hat{\rho}^{ABCD} = |\Psi\rangle\langle\Psi|$ with respect to subsystem A is constructed by using the condition

$$\langle i_1 i_2 i_3 i_4 | \hat{\rho}_G^{TA} | j_1 j_2 j_3 j_4 \rangle = \langle j_1 i_2 i_3 i_4 | \hat{\rho}^{ABCD} | i_1 j_2 j_3 j_4 \rangle. \quad (32)$$

The K -way partial transpose ($2 \leq K \leq 4$) of state operator $\hat{\rho}^{ABCD}$ with respect to subsystem A is defined as

$$\langle i_1 i_2 i_3 i_4 | \hat{\rho}_K^{TA} | j_1 j_2 j_3 j_4 \rangle = \langle j_1 i_2 i_3 i_4 | \hat{\rho}^{ABCD} | i_1 j_2 j_3 j_4 \rangle \quad \text{if} \quad \sum_{m=1}^N (1 - \delta_{i_m, j_m}) = K, \quad (33)$$

and

$$\langle i_1 i_2 i_3 i_4 | \hat{\rho}_K^{TA} | j_1 j_2 j_3 j_4 \rangle = \langle i_1 i_2 i_3 i_4 | \hat{\rho}^{ABCD} | j_1 j_2 j_3 j_4 \rangle \quad \text{if} \quad \sum_{m=1}^N (1 - \delta_{i_m, j_m}) \neq K,$$

where

$$\begin{cases} \delta_{i_m, j_m} = 1 \text{ for } i_m = j_m \\ \delta_{i_m, j_m} = 0 \text{ for } i_m \neq j_m \end{cases}. \quad (34)$$

Similar constraints are applied to construct global and K -way partial transpose with respect to subsystems B , C or D . The negativity of ρ^{T_p} is related to the trace norm of ρ^{T_p} through

$$N^p = \frac{1}{d_p - 1} (\|\rho^{T_p}\|_1 - 1). \quad (35)$$

Negativity based on Peres Horodecki criterion is a natural entanglement measure. We define the global negativity with respect to subsystem p as

$$N_G^p = \frac{1}{d_p - 1} (\|\rho_G^{T_p}\|_1 - 1), \quad (36)$$

and K -way negativity [27, 29] as

$$N_K^p = \frac{1}{d_p - 1} (\|\rho_K^{T_p}\|_1 - 1), \quad (37)$$

where d_p is the dimension of the Hilbert space associated with subsystem p .

Furthermore, we define 3-way partial transpose $\hat{\rho}_3^{T_{A-ABC}}$ involving the qubits ABC as

$$\begin{aligned} \langle i_1 i_2 i_3 i_4 | \hat{\rho}_3^{T_{A-ABC}} | j_1 j_2 j_3 j_4 \rangle &= \langle j_1 i_2 i_3 i_4 | \hat{\rho}^{ABCD} | i_1 j_2 j_3 j_4 \rangle \\ \text{if } \sum_{m=1}^4 (1 - \delta_{i_m, j_m}) &= 3, \text{ and } i_1 \neq j_1, \end{aligned} \quad (38)$$

$$\begin{aligned} \langle i_1 i_2 i_3 i_4 | \hat{\rho}_K^{T_{A-ABC}} | j_1 j_2 j_3 j_4 \rangle &= \langle i_1 i_2 i_3 i_4 | \hat{\rho}^{ABCD} | j_1 j_2 j_3 j_4 \rangle \\ \text{if } \sum_{m=1}^4 (1 - \delta_{i_m, j_m}) &= 3, \text{ and } i_1 = j_1, \end{aligned} \quad (39)$$

and

$$\langle i_1 i_2 i_3 i_4 | \hat{\rho}_K^{T_{A-ABC}} | j_1 j_2 j_3 j_4 \rangle = \langle i_1 i_2 i_3 i_4 | \hat{\rho}^{ABCD} | j_1 j_2 j_3 j_4 \rangle \quad \text{if } \sum_{m=1}^4 (1 - \delta_{i_m, j_m}) \neq 3, \quad (40)$$

with the corresponding negativity

$$N_3^{A-ABC} = \frac{1}{d_p - 1} \left(\left\| \hat{\rho}_3^{T_{A-ABC}} \right\|_1 - 1 \right). \quad (41)$$

Analogous definitions hold for the 3-way partial transposes $\hat{\rho}_3^{T_{A-ABD}}$, $\hat{\rho}_3^{T_{A-ACD}}$, and $\hat{\rho}_3^{T_{D-BCD}}$.

B. Global and partial K -way negativity

Global negativity with respect to a subsystem can be written as a sum of partial K -way negativities. The global transpose with respect to subsystem p , written in its eigen basis is given by

$$\hat{\rho}_G^{T_p} = \sum_i \lambda_i^{G+} |\Psi_i^{G+}\rangle \langle \Psi_i^{G+}| + \sum_i \lambda_i^{G-} |\Psi_i^{G-}\rangle \langle \Psi_i^{G-}|, \quad (42)$$

where λ_i^{G+} and $|\Psi_i^{G+}\rangle$ (λ_i^{G-} and $|\Psi_i^{G-}\rangle$) are the positive (negative) eigenvalues and eigenvectors of $\hat{\rho}_G^{T_p}$, respectively. Using the definition of trace norm and $\text{Tr}(\hat{\rho}_G^{T_p}) = 1$, the negativity of $\hat{\rho}_G^{T_p}$ is given by

$$N_G^p = -\frac{2}{d_p - 1} \sum_i \langle \Psi_i^{G-} | \hat{\rho}_G^{T_p} | \Psi_i^{G-} \rangle = -\frac{2}{d_p - 1} \sum_i \lambda_i^{G-}. \quad (43)$$

The global transpose with respect to subsystem p , may also be rewritten as

$$\hat{\rho}_G^{T_p} = \sum_{K=2}^N \hat{\rho}_K^{T_p} - (N-2)\hat{\rho}. \quad (44)$$

Substituting Eq. (44) in Eq. (43), we get

$$-2 \sum_i \lambda_i^{G-} = -2 \sum_{K=2}^N \sum_i \langle \Psi_i^{G-} | \hat{\rho}_K^{T_p} | \Psi_i^{G-} \rangle + 2(N-2) \sum_i \langle \Psi_i^{G-} | \hat{\rho} | \Psi_i^{G-} \rangle. \quad (45)$$

Defining partial K -way negativity E_K^p ($K = 2$ to N) as

$$E_K^p = -\frac{2}{d_p - 1} \sum_i \langle \Psi_i^{G-} | \hat{\rho}_K^{T_p} | \Psi_i^{G-} \rangle, \quad (46)$$

and

$$E_0^p = -\frac{2(N-2)}{d_p - 1} \sum_i \langle \Psi_i^{G-} | \hat{\rho} | \Psi_i^{G-} \rangle \quad (47)$$

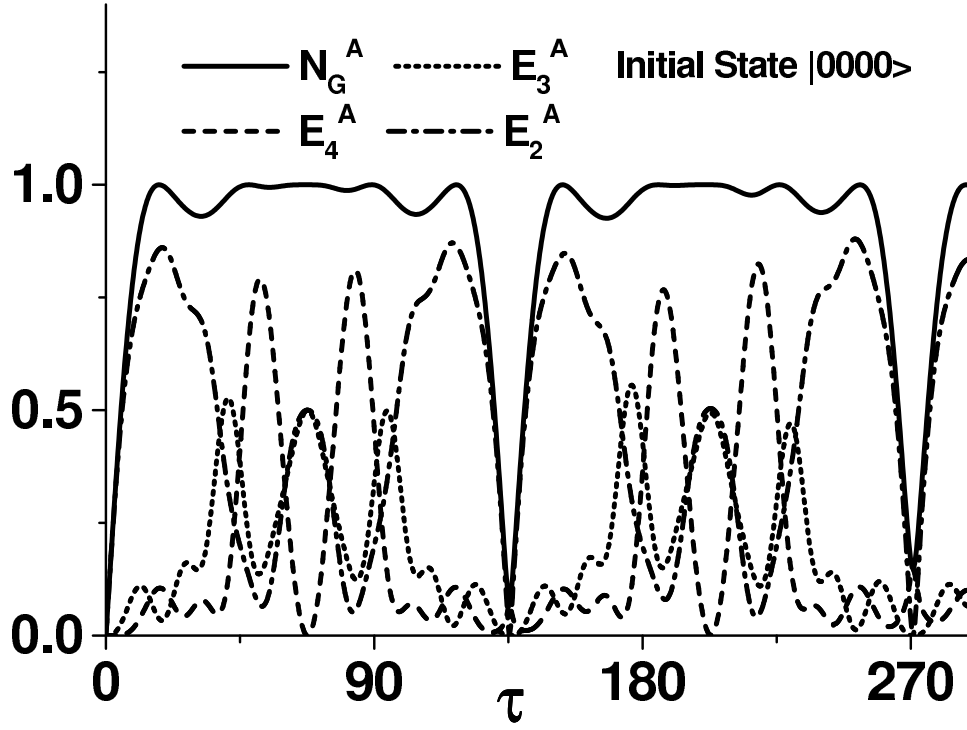


FIG. 3: The global negativity N_G^A , and entanglement measures E_K^A , for $K = 2$ to 4 versus $\tau (= g\eta t)$ for the initial state $|0000\rangle$.

we may split the global negativity for qubit p as

$$N_G^p = \sum_{K=2}^N E_K^p - E_0^p. \quad (48)$$

To obtain tripartite GHZ state like correlations between three subsystems, we calculate

$$E_3^{A-ABC} = -\frac{2}{d_p - 1} \sum_i \langle \Psi_i^{G-} | \hat{\rho}_3^{T_{A-ABC}} | \Psi_i^{G-} \rangle, \quad (49)$$

$$E_3^{A-ABD} = -\frac{2}{d_p - 1} \sum_i \langle \Psi_i^{G-} | \hat{\rho}_3^{T_{A-ABD}} | \Psi_i^{G-} \rangle, \quad (50)$$

and

$$E_3^{A-ACD} = -\frac{2}{d_p - 1} \sum_i \langle \Psi_i^{G-} | \hat{\rho}_3^{T_{A-ACD}} | \Psi_i^{G-} \rangle. \quad (51)$$

It is easily verified that for the system at hand $E_3^{A-ABC} = 0$, and $E_3^{A-ACD} = E_3^{A-ABD} = E_3^A/2.0$. As such the three qubits have no genuine tripartite entanglement.

C. Entanglement dynamics of the pure state $\Psi_{m+1,n+1}(t)$

We use the global negativity to detect the entanglement of parts in bipartite splits of the system. In case the negativities N_G^A , N_G^B , N_G^C , N_G^D and N_G^{AB} are non zero, the system has 4-partite entanglement. The 4-way, 3-way and 2-way partial negativities identify and quantify the different types of entanglement between the subsystems of the composite system in a given state. From the state operator $\hat{\rho}(t) = |\Psi_{m+1,n+1}(t)\rangle \langle \Psi_{m+1,n+1}(t)|$, the global and K -way partial transposes are constructed by following the prescription given in section IV (Eq. (32) and Eq. (33)). The state of Eq. (13) is very special in that analytical results can be obtained for partial K -way negativities

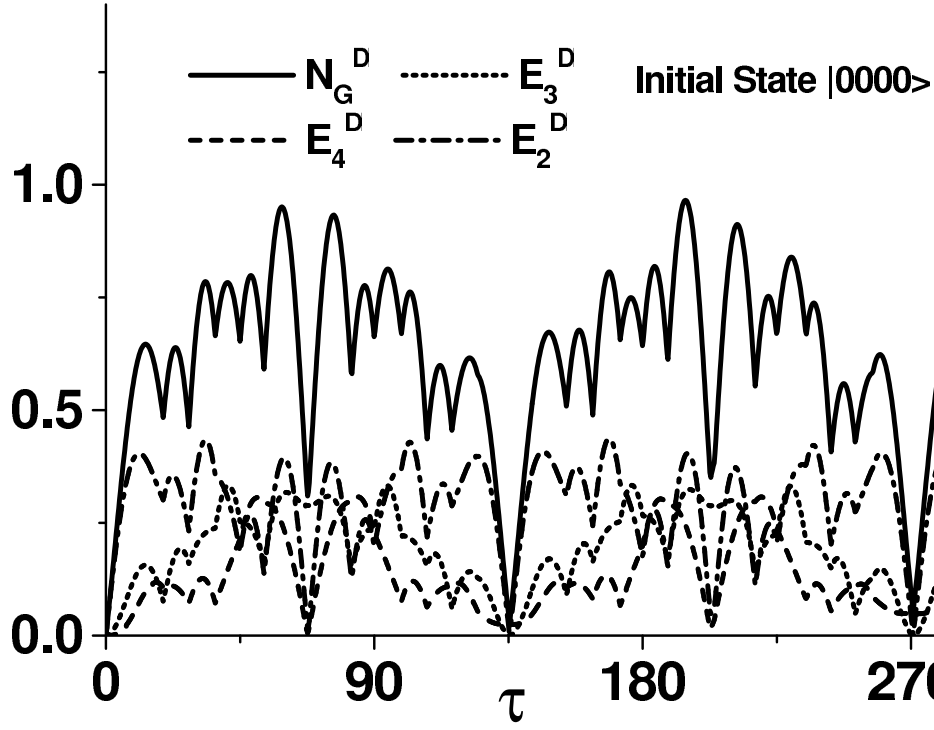


FIG. 4: The global negativity N_G^D , and entanglement measures E_K^D , for $K = 2$ to 4 versus $\tau (= g\eta t)$ for the initial state $|0000\rangle$.

characterizing the state. Using negative eigen functions of $\rho_G^{T_p}$, the entanglement measures E_K^p for $K = 2, 3$ and 4 are easily obtained. The negativity of global partial transpose with respect to qubit A is found to be

$$N_G^A = 2 \sqrt{\left(|a_0(t)|^2 + \frac{2|a_1(t)|^2}{3} + \frac{|a_2(t)|^2}{3} \right) \left(|a_3(t)|^2 + \frac{|a_1(t)|^2}{3} + \frac{2|a_2(t)|^2}{3} \right)}. \quad (52)$$

Using the eigenvector corresponding to the negative eigenvalue of $\rho_G^{T_A}$, we get the partial negativities

$$E_4^A = \frac{4}{N_G} \left(|a_0(t)|^2 |a_3(t)|^2 + \frac{|a_1(t)|^2 |a_2(t)|^2}{3} \right), \quad (53)$$

$$E_3^A = \frac{4}{N_G} \left(\frac{2|a_0(t)|^2 |a_2(t)|^2}{3} + \frac{2|a_1(t)|^2 |a_3(t)|^2}{3} \right), \quad (54)$$

and

$$E_2^A = \frac{4}{N_G} \left[\frac{|a_0(t)|^2 |a_1(t)|^2}{3} + \frac{|a_2(t)|^2 |a_3(t)|^2}{3} + 2 \left(\frac{|a_1(t)|^2}{3} + \frac{|a_2(t)|^2}{3} \right)^2 \right]. \quad (55)$$

It is easily seen that $N_G^A = N_G^B = N_G^C$. Next we construct the transposes $\rho_G^{T_D}$, $\rho_4^{T_D}$, $\rho_3^{T_D}$, and $\rho_2^{T_D}$, for the decomposition $ABC - D$ of the state $\Psi_{m+1,n+1}(t)$ and obtain

$$\begin{aligned} N_G^D &= \frac{2}{3} |a_0(t)| (|a_1(t)| + |a_2(t)| + |a_3(t)|) \\ &\quad + \frac{2}{3} |a_1(t)| (|a_2(t)| + |a_3(t)|) + 2 |a_2(t)| |a_3(t)|, \end{aligned} \quad (56)$$

$$E_4^D = \frac{2}{3} |a_0(t)| |a_3(t)| + \frac{2}{9} |a_1(t)| |a_2(t)|, \quad (57)$$

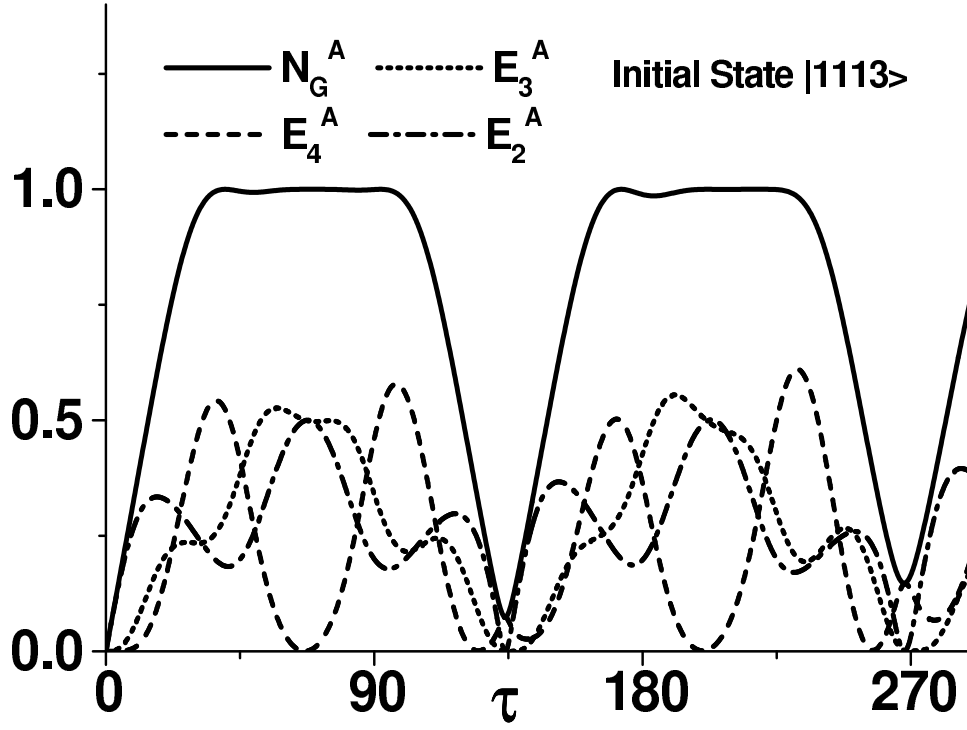


FIG. 5: The global negativity N_G^A , and entanglement measures E_K^A , for $K = 2$ to 4 versus $\tau (= g\eta t)$ for the initial state $|1113\rangle$.

$$E_3^D = \frac{2}{3} |a_0(t)| |a_2(t)| + \frac{2}{3} |a_1(t)| |a_3(t)|, \quad (58)$$

and

$$E_2^D = \frac{2}{3} |a_0(t)| |a_1(t)| + \frac{2}{3} |a_2(t)| |a_3(t)| + \frac{4}{9} |a_1(t)| |a_2(t)|. \quad (59)$$

Since the three qubits have no genuine tripartite entanglement, the partial negativity E_3^D represents the entanglement of quantum system D with the W like states of three qubits.

Treating AB as a single system in Hilbert space of dimension four, the global negativity is found to be

$$N_G^{AB} = \frac{2}{3} (\mu_0 \mu_1 + \mu_0 \mu_2 + \mu_1 \mu_2), \quad (60)$$

where

$$\begin{aligned} \mu_0 &= \sqrt{|a_0(t)|^2 + \frac{|a_1(t)|^2}{3}}, & \mu_1 &= \sqrt{\frac{2|a_1(t)|^2}{3} + \frac{2|a_2(t)|^2}{3}}, \\ \mu_2 &= \sqrt{|a_3(t)|^2 + \frac{|a_2(t)|^2}{3}}. \end{aligned} \quad (61)$$

Figures (3) and (4) display the global negativity and K -way entanglement of qubits A and D in the state $\Psi_{33}(t)$, as a function of interaction parameter $\tau = g\eta t$. At $\tau \approx \frac{3\pi}{8}$, we have $E_3^A = E_2^A = 0.5$, indicating that the qubit A (or B or C), has equally strong bipartite and tripartite correlations. Recalling that no genuine tripartite entanglement exists between the three qubits as evidenced by $E_3^{A-ABC} = 0$, we have here the three qubits in W_1 -like state entangled to the subsystem D . In other words, the cavity field is entangled to three ions in W_1 -like state and can be used to transfer the entanglement of the composite system to a remote quantum system. The probability plot of figure (1) confirms that for interaction time $t = \frac{3\pi}{8g\eta}$, $P_0(\tau) = P_2(\tau) = 0$, $P_1(\tau)$ shows a peak and $P_3(\tau)$ is finite. A measurement that finds the cavity in two photon state collapses the composite system state to three ions in W_1 -state with center of mass in two phonon state.

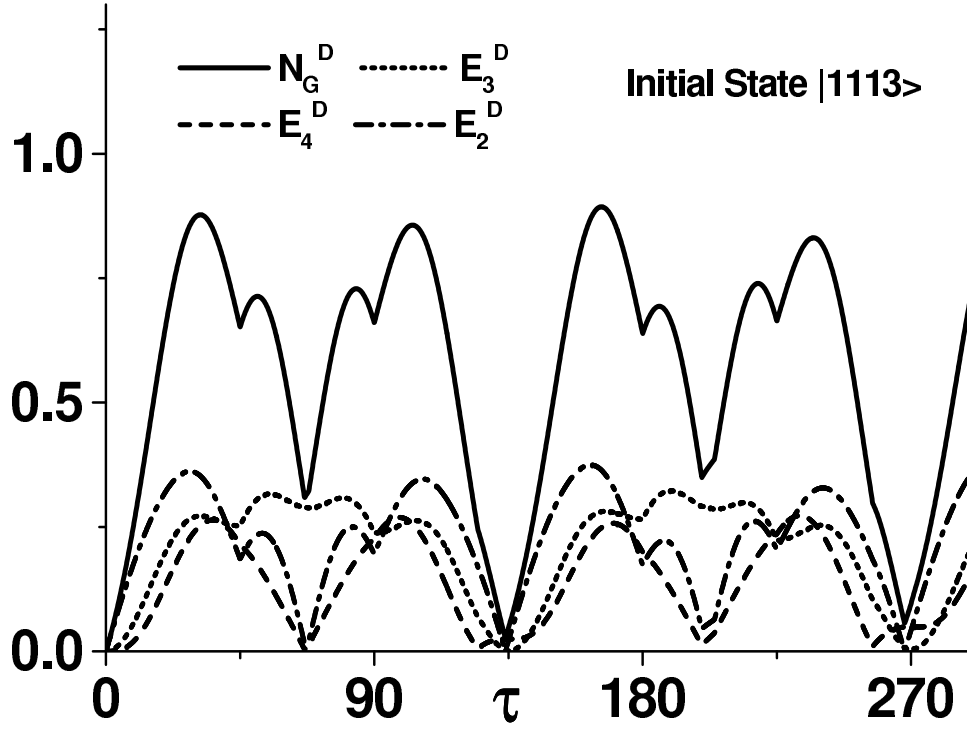


FIG. 6: The global negativity N_G^D , and entanglement measures E_K^D , for $K = 2$ to 4 versus $\tau (= g\eta t)$ for the initial state $|1113\rangle$.

D. Entanglement dynamics of the pure state $\Phi_{m-2,n-2}(t)$

Analytical expressions for negativities and partial K -way negativities for the state $\Phi_{m-2,n-2}(t)$ (Eq. (21)), written in computational basis as

$$\begin{aligned} \Phi_{m-2,n-2}(t) = & a_3(t)|0000\rangle + a_2(t) \left(\frac{|1001\rangle + |0101\rangle + |0011\rangle}{\sqrt{3}} \right) \\ & + a_1(t) \left(\frac{|1102\rangle + |1012\rangle + |0112\rangle}{\sqrt{3}} \right) + a_0(t)|1113\rangle. \end{aligned} \quad (62)$$

are analogous to those for the state $\Psi_{m+1,n+1}(t)$. For the special case of state $\Phi_{00}(t)$, the global and partial K -way negativities are displayed, in Figs. (5) and (6) for qubits A and D , respectively. The negativities N_G^{AB} for the states $\Psi_{33}(t)$ and $\Phi_{00}(t)$ are shown in Fig. (7). At $\tau = \frac{3\pi}{8}$, the coefficient $a_2(t) = a_0(t) = 0$, and $E_3^A = E_2^A = 0.5$ giving (using Eq. 22) the state

$$\Phi_{00}(\tau = \frac{3\pi}{8}) = a_3(t)|000, m+1, n+1\rangle + a_1(t)|W_2, m-1, n-1\rangle,$$

In this case we have three ions in W_2 -like state entangled to photon-phonon system. As such detecting the cavity in single photon state ensures that the three ions are in W_2 state. The entanglement of the cavity field with three ions in W_2 -like state may, on the other hand, be used to communicate with a remote quantum system. For an interaction time $t = \frac{3\pi}{8g\eta}$, $P_2(\tau)$ shows a peak and $P_0(\tau)$ is finite in the probability plot of figure (2).

The number of initial state vibrational quanta also controls the nature of entanglement in the composite system states. We notice that for a single phonon initial state the general form of the state (Eq. (23))

$$\Psi_{1,n+1}(t) = a_0(t)|0000\rangle + a_1(t) \left(\frac{|1001\rangle + |0101\rangle + |0011\rangle}{\sqrt{3}} \right), \quad (63)$$

allows only bipartite entanglement. For $m \geq 2$, the composite system may have genuine 4-partite, tripartite as well as bipartite entanglement. This is an interesting aspect unique to systems where vibrational motion of ions is coupled to cavity field.

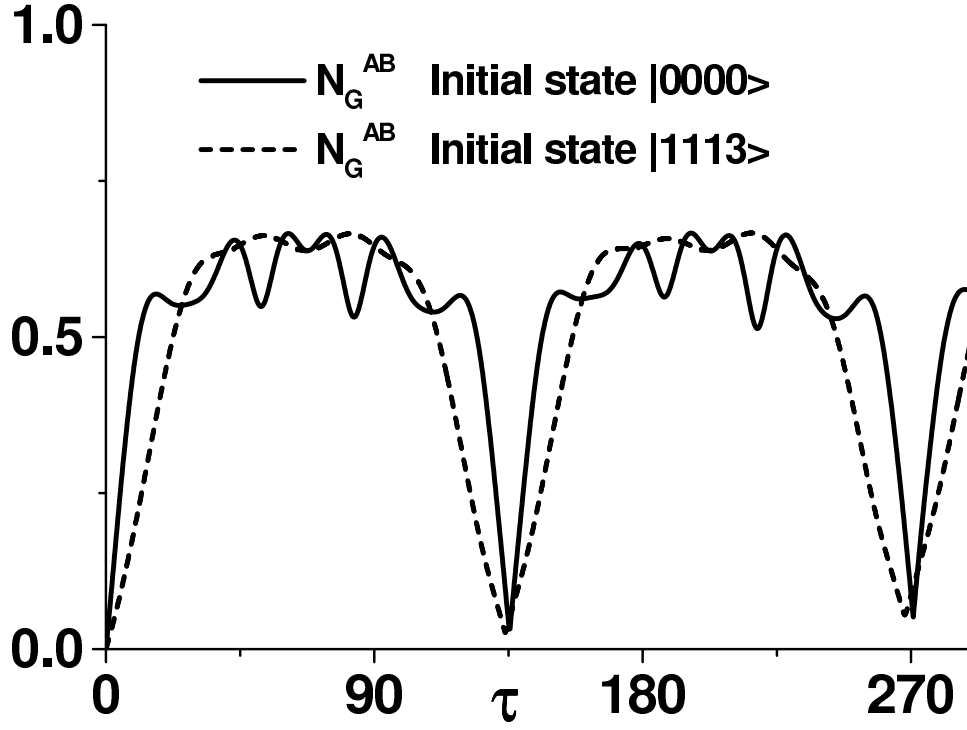


FIG. 7: The global negativity N_G^{AB} versus $\tau(=g\eta t)$ for the initial states $|0000\rangle$ and $|1113\rangle$.

V. WHAT DO THE K -WAY NEGATIVITIES ADD TO OUR KNOWLEDGE OF THE SYSTEM?

Figures (3-7) show the entanglement distribution between possible entanglement modes available to the system in states $\Psi_{33}(t)$ and $\Phi_{00}(t)$. Since analytical expressions for partial K -way negativities are available for specific initial state preparations, the rate of change of partial K -way negativity for a particular mode can be easily obtained, if needed. The two way partial negativity is seen to grow at the fastest rate being the first to reach its peak value, followed by two peaks showing maxima of partial 3-way and 4-way negativities, respectively. Besides that a reversible entanglement exchange between different entanglement modes is observed. In Fig. (3) at the maxima of partial 4-way negativity, partial 2-way and 3-way negativities are rather small, whereas the minima of E_4^A correspond to a large contribution to total entanglement from bipartite and genuine tripartite entanglement. Similar trend is seen in Figures (4-6). Figure (7) complements the information about entanglement distribution obtained from Figures (1-6). Once the interaction is switched on, a typical qubit pair is found to be in an entangled state until the composite becomes separable again. As seen from the global negativity plots, the period after which the composite system becomes separable is given by $T = \frac{3\pi}{4g\eta}$.

In particular, we look at the entanglement of states $\Psi_{m+1,n+1}^{W_1}$ (Eq. (18)) and $\Phi_{m-2,n-2}^{W_2}$ (Eq. (22)). For both types of states $N_G^D = E_3^D$, that is there is no genuine four partite entanglement amongst the subsystems A, B, C and D . The global negativities are however finite for A, B, C, D as well as AB , pointing to four partite entanglement. Although for qubits A, B , and C we get finite partial 2-way negativities, four partite entanglement cannot be due to two-way correlations because $E_2^D = 0$. The 2-way negativity of the partial transpose of W_1 state or W_2 state is 0.94, whereas the three way negativity is zero. As such a W state is a state with maximal tripartite entanglement generated by 2-way correlations. In states $\Psi_{m+1,n+1}^{W_1}$ and $\Phi_{m-2,n-2}^{W_2}$ ions in a W like state are entangled to subsystem D . We conclude that the four-partite entanglement of three ions with photon-phonon system is generated by 2-way and 3-way correlations.

VI. CONCLUSIONS

We have studied the entanglement dynamics of spatially separated three two-level cold trapped ions in a high finesse cavity with the cavity tuned to the red sideband of ionic vibrational motion. Analytical expressions for the state of composite system as a function of interaction time are obtained for interaction Hamiltonian of Eq. 3 with

the cavity prepared initially in different photon number states. With three ions initially in their ground state, the state $|000, m+1, n+1\rangle$ evolves (i) for $m = 0$ and $n \geq 0$, in a bi-dimensional subspace, (ii) for $m = 1$ and $n \geq 1$ in a tridimensional subspace, and (iii) for $m \geq 2$ and $n \geq 2$ in a four-dimensional subspace of the coupled basis ionic states. The initial state $|111, m+1, n+1\rangle$ always evolves in a four-dimensional subspace independent of the initial phonon and photon number. The number of initial state vibrational quanta offers a control mechanism for manipulation of composite system states, when ions are in their ground state initially. This is an interesting aspect unique to systems where vibrational motion of ions is coupled to cavity field in contrast to the ions coupled only to quantized cavity field [33], [34] or only with the vibrational modes [35]. Useful practical applications to implement information processing and communication related tasks, can benefit from this special feature. The reduced three ion state operator is obtained by tracing out the phonon and photon degrees of freedom. For cavity ion coupling strength $g = 8.95$ MHz, Lamb Dicke parameter value $\eta = 0.01$ and cavity prepared in single photon state at $t = 0$, the minimum interaction time needed generate a three ion W-state is found to be $\sim 10.133\mu$ sec. For the initial state in which three ions are in their ground state and center of mass in two phonon state, the W_2 state generation probability increases while the minimum interaction time to get the probability peak decreases, with increase in the number of photons present in the cavity at $t = 0$.

The ionic qubits in W state are found to be entangled to cavity photons, that may be used to transport information to a remote cavity in a fast and reliable way. Multipartite entanglement dynamics of the composite system is examined using global, four-way, three-way and two-way negativities. Analytical expressions for partial K -way negativities ($K = 2$ to 4) are obtained. For the three ions prepared initially in their ground state or in their excited state, the partial K -way negativities are calculated numerically and plotted as a function of interaction parameter. These plots show the entanglement distribution as well as the rate of change with time of entanglement between possible entanglement modes available to the system. Besides that reversible entanglement exchange between different entanglement modes is observed. For specific values of interaction parameter, the three ions and photon-phonon system are found to have four partite entanglement, generated by 2-way and 3-way correlations. Three ions in W state are found to be entangled to photons. We expect this analysis to add to the understanding of multipartite entanglement in the context of trapped ions interacting with photons in optical cavities.

Acknowledgments

S. S. Sharma acknowledges financial support from FAEP/Uel, and Fundação Araucaria PR, Brazil. E. de Almeida thanks Capes, Brazil for financial support.

-
- [1] A. K. Ekert, Phys. Rev. Lett. **67**, 661 (1991).
 - [2] C. H. Bennett and S. J. Wiesner, Phys. Rev. Lett. **69**, 2881 (1992).
 - [3] C. H. Bennett, G. Brassard, C. Crepeau, R. Jozsa, A. Peres, and W. K. Wootters, Phys. Rev. Lett. **70**, 1895 (1993).
 - [4] C. Monroe, D. M. Meekhof, B. E. King, W. M. Itano and D. J. Wineland, Phys. Rev. Lett. **75**, 4714 (1995).
 - [5] D. J. Wineland, C. Monroe, W. M. Itano, D. Leibfried, B. E. King, and D. M. Meekhof, NIST J. Res. **103**, 259 (1998).
 - [6] C. F. Roos, Th. Zeiger, H. Rohde, H. C. Nagerl, J. Eschner, D. Leibfried, F. Schmidt-Kaler, R. Blatt, Phys. Rev. Lett. **83**, 4713 (1999). C. Monroe, D. M. Meekhof, B. E. King, W. M. Itano and D. J. Wineland, Phys. Rev. Lett. **75**, 4714 (1995).
 - [7] H. Häffner, W. Hänsell, C. F. Roos, J. Benhelm, D. Chek-al-kar, M. Chwalla, T. Körber, U. D. Rapol, M. Riebe, P. O. Schmidt, C. Becher, O. Gühne, W. Dür and R. Blatt, Nature 438, 643 (2005).
 - [8] J.I. Cirac et al., Phys. Rev. Lett. **78**, 3221 (1997).
 - [9] V. Buzek, G. Drobny, M. S. Kim, G. Adam, and P. L. Knight, Phys. Rev. A **56**, 2352 (1997).
 - [10] S. Shelly Sharma, Phys. Lett. A **311**, 187 (2003).
 - [11] S. Shelly Sharma, N. K. Sharma and E. de Almeida, J. Phys. B: At. Mol. Opt. phys. **39** 695(2006).
 - [12] A. B. Mundt, A. Kreuter, C. Becher, D. Leibfried, J. Eschner, F. Schmidt-Kaler, R. Blatt, Phys. Rev. Lett. **89**, 103001 (2002).
 - [13] A. B. Mundt, A. Kreuter, C. Russo, C. Becher, D. Leibfried, J. Eschner, F. Schmidt-Kaler, R. Blatt, Appl. Phys. B **76**, 117 (2003).
 - [14] J. Eschner, Ch. Raab, A. Mundt, A. Kreuter, C. Becher, F. Schmidt-Kaler, and R. Blatt, Fortschr. Phys. **51**, 359 (2003).
 - [15] G. Morigi, J. Eschner, and C. H. Keitel, Phys. Rev. Lett. **85**, 4458 (2000).
 - [16] C. F. Roos, D. Leibfried, A. B. Mundt, F. Schmidt-Kaler, J. Eschner, R. Blatt, Phys. Rev. Lett. **85**, 5547 (2000).
 - [17] T. E. Tessier, I. H. Deutsch, and A. Delgado, Physical Review A **68**, 062316 (2003).
 - [18] Tavis and F.W. Cummings, Phys. Rev. **170**, 379 (1968).
 - [19] C. Di Fidio, S. Maniscalco, and W. Vogel, Phys. Rev. A, **65**, 033825 (2002).
 - [20] D. Bouwmeester, A. Ekert, and A. Zeilinger, The Physics of Quantum Information (Berlin: Springer) (2000).
 - [21] K. Zyczkowski, P. Horodecki, A. Sanpera, and M. Lewenstein, Phys. Rev. A **58**, 883 (1998).
 - [22] G. Vidal, J. Mod. Opt. **47**, 355 (2000).
 - [23] J. Eisert, PhD thesis (University of Potsdam, February 2001).

- [24] A. Peres Phys. Rev. Lett. 77, 1413(1996).
- [25] M. Horodecki, P. Horodecki, and R. Horodecki, Phys. Lett. A 223, 1(1996).
- [26] G. Vidal and R. F. Werner, Phys. Rev. Vol. 65, 032314 (2002).
- [27] S. S. Sharma, and N. K. Sharma, quant-ph/0608062 (unpublished).
- [28] S. S. Sharma, and N. K. Sharma, Phys. Rev. A 76, 012326 (2007).
- [29] S. S. Sharma, and N. K. Sharma, Phys. Rev. A 77, 042117 (2008).
- [30] S. S. Sharma, A. Vidiella-Barranco, Phys. Lett. A 309, 345 (2003).
- [31] S. S. Sharma, and N. K. Sharma, arXiv:0806.0887v1 [quant-ph].
- [32] V. Coffman, J. Kundu, and W. K. Wootters, Phys. Rev. A 61, 052306 (2000).
- [33] K. Fujii, K. Higashida, R. Kato, T. Suzuki, and Y. Wada, Int. Jour. of Geometric Methods in Modern Physics **1**, 6 (2004).
- [34] JF. Cai and HP. Liu, Commun. Theor. Phys. **43**, 3, 427 - 431 (2005).
- [35] A. Retzker, E. Solano and B. Reznik, Phys. Rev. A 75, 022312 (2007).